Int. J. Nano Dimens., 8 (3): 257-264, Summer 2017

ORIGINAL ARTICLE

Synthesis and characterization of superparamagnetic Iron Oxide nanoparticles (SPIONs) stabilized by Glucose, Fructose and Sucrose

*Dhananjayan Sivakumar[1, 2]; Mehboob Mohamed Rafi[2]; Balaraman Sathyaseelan[3]; Kulam Mohammed Prem Nazeer [2, *]; Ahmed Meeran Ayisha Begam[4]*

[1]*Department of Physics, Sree Krishna College of Engineering, Unai, Anaicut, Tamilnadu, India*
[2]*PG and Research Department of Physics, Islamiah College, Vaniyambadi, Tamilnadu, India*
[3]*Department of Physics, University College of Engineering-Arni, Tamilnadu, India*
[4]*Department of Physics, Avinashilingam Institute for Home Science and Higher Education, Coimbatore, Tamilnadu, India*

Received 10 April 2017; revised 29 June 2017; accepted 08 July 2017; available online 14 July 2017

Abstract

The aim of this study is to obtain polysaccharide (Glucose, Fructose and Sucrose) stabilized superparamagnetic iron oxide nanoparticles (SPIONs) by Co-Precipitation method. As prepared iron oxide nanoparticles have been characterized by X-ray Diffraction (XRD), Fourier Transform infrared (FTIR) spectroscopy, UV–Vis NIR spectroscopy, High Resolution Transmission Electron Microscope (HRTEM) and Vibrating Sample Magnetometer (VSM). The average crystallite sizes as determined from XRD for Glucose–Fe_3O_4 (GF), Fructose–Fe_3O_4 (FF) and Sucrose–Fe_3O_4 (SF) are 3.3, 4.82 and 5.23 nm, respectively. Powder XRD study also demonstrates that the synthesized nanoparticles are indexed for spinel cubic lattice. FTIR spectrum shows a good vibrational interaction between Fe_3O_4 and polysaccharides functional groups and it controls the growth of Fe_3O_4 nanoparticles. SPIONs exhibit superparamagnetic properties with a coercivity ranging from 0.55 to 9.13 Oe and a saturation magnetization in the range 38-42 emu/g.

Keywords: *HRTEM; Magnetic properties; Polysaccharides; SPIONs; VSM.*

How to cite this article

Sivakumar D, Mohamed Rafi M, Sathyaseelan B, Prem Nazeer K, Ayisha Begam A. Synthesis and characterization of superparamagnetic Iron Oxide nanoparticles (SPIONs) stabilized by Glucose, Fructose and Sucrose. Int. J. Nano Dimens., 2017; 8 (3): 257-264.

INTRODUCTION

Iron oxide (Fe_3O_4) nanoparticles (also termed as magnetite) have attracted much interest due to its useful applications in biomedical imaging and cell tracking. Magnetite (Fe_3O_4) and its oxidized form (γ-Fe_2O_3) are the most studied [1-3] and it has unique magnetic properties with good biocompatibility at nano regime [4-5].

The demanding properties of magnetic particles that lead to biological and biomedical applications are controlled particle size, biocompatibility, non-toxicity, narrow and moderate size distribution, high crystallinity, large surface area and ability to disperse in an aqueous medium [6-9]. In order to satisfy these criteria many researcher have studied and developed stable, nontoxic, and economically viable magnetic nanoparticles [10-12]. Encapsulating magnetic nanoparticles within a polymer coating not only stabilizes the nanoparticles but also provides various chemical functionalizations. Many polysaccharide-based magnetic nano-composites such as magnetite (Fe_3O_4)-dextran, Fe_3O_4-chitosan, Fe_3O_4-alginate, Fe_3O_4-heparin, Fe_3O_4-pullulan acetate, were successfully used in the bio-separation and purification [13-14].

The present work is on the synthesis of Superparamagnetic iron oxide nanoparticles (SPIONs) in presence of Polysaccharide based stabilizers (Glucose, Fructose and Sucrose) using Co-precipitation method. As prepared iron oxide nano powder, they have been subjected to X-ray

* Corresponding Author Email: *sivakumar6580@gmail.com*

diffraction to determine its crystalline phase and average particle size. The microstructure and the particle size distribution were analyzed through High Resolution Transmission electron microscopy (HRTEM). Magnetization measurement was done at room temperature by using Vibrating Sample Magnetometer studies (VSM).

EXPERIMENTAL

Materials

Polysaccharides (Glucose, Fructose and Sucrose) were purchased obtained from Sigma-Aldrich. The reagents Iron chloride hexahydrate ($FeCl_3.6H_2O$) $FeSO_4.7H_2O$, $NH_3.H_2O$ used were analytical grade.

Preparation of Glucose–Fe_3O_4 (GF), Fructose–Fe_3O_4 (FF) and Sucrose–Fe_3O_4 (SF)

Measured weight of 1.2 g polysaccharide (Glucose) was dissolved in 200 ml of distilled water and continuously stirred for 10 min at 90°C for the dissolution of polysaccharide. The solution was subsequently cooled to room temperature and aqueous solutions of $FeCl_3 \cdot 6H_2O$ (1.49g) and $FeSO_4 \cdot 7H_2O$ (0.765g) were used in the preparations. The mixed solution was then heated at 60°C under nitrogen atmosphere. Ammonia–water mix (8mol) was added dropwise to obtain a solution pH of the final mixture in the range of 11. The final solution was held at 60°C for 4 h and the suspension was then centrifuged at 11,000 rpm for 10 min. The experiment is repeated for other polysaccharide (Fructose, Sucrose). The settled polysaccharide Fe_3O_4 nanoparticles were washed three times using distilled water to remove by products and excess polysaccharides. The product was again washed two times with distilled water and then with ethanol. At the end the sample was dried in an oven at 100°C for 3 hrs and labeled as GF, FF and SF, respectively.

Characterization

The crystal structure of the obtained products was characterized by X-ray Diffraction (XRD) Bruker Model: D8 advance diffractometer with CuK_α radiation (k=1.5406 Å) operating at 40 kV and 30 mA. IR spectra were obtained using a BRUKER 10049391 IR Spectrometer instrument at room temperature in the 4000-500 cm^{-1} ranges. The UV-Visible NIR spectra of the sample were taken in wavelength range from 200 to 2500 nm using Varian Cary 5000 spectrophotometer. High Resolution Transmission Electron Microscope (HRTEM) JEOL JEM 2100 was used for characterizing the size of nanoparticles. The magnetic properties of the samples were studied by Vibrating Sample Magnetometers (VSM) Lakeshore 7410 at room temperature.

RESULTS AND DISCUSSION

X-ray Diffraction Analysis

The comparative powder X-ray diffraction patterns of the GF, FF and SF are shown in Fig. 1. All the peaks of XRD patterns were analyzed and indexed (JCPDS No.85-1436) and compared with magnetite standards [15, 16]. The samples exhibited very broad peaks indicating the fine and small crystallite size of particles. The strongest reflection peaks from (311) planes, the characteristic of cubic spinel phase [17]. The other peaks indexed as (220), (311), (400), (333) and (440) planes correspond also to a cubical ones [18, 19]. The average crystallite size of nanoparticles could be estimated using Debye Scherrer formula $D= k\lambda/\beta\cos\theta$, where D is the crystallite mean size, k is a shape function for which a value of 0.9 is normally used, λ is the wavelength of the radiation, β is the full width at half- maximum (FWHM) in the 2θ scale and θ is the Bragg angle [20]. It was found that the average crystallite size were 3.3, 4.82 and 5.23 nm for GF, FF and SF respectively.

FTIR analysis

FTIR spectra recorded for GF, FF and SF in the range between 4000–500 cm^{-1} are shown in Fig. 2 (a-c). The spectra gave information about the chemical and molecular structure changes in the synthesized GF, FF and SF. In the finger print region of the fructose stabilized sample (Fig. 2 (b)) there were three characteristic peaks of –C–O– stretching. The peak at 1163 cm^{-1} was ascribed to C–O bond stretching in the C–O–H group, and two other peaks at 1527 and 1020 cm^{-1} were attributed to C–O bond stretching of the C–O–C group in the anhydroglucose ring [21].

In FTIR spectrum of FF (Fig. 2 (b)), a high intensity broad band appeared at around 629 cm^{-1} which may be due to the Fe_3O_4 [22]. The –C–O– stretching peaks of fructose found to have been shifted in the presence of Fe_3O_4 medium indicating that a strong interaction could be existing between the fructose and Fe_3O_4 [23]. In the FTIR spectrum of Glucose and Sucrose (Fig. 2(a), 2(c)) based Fe_3O_4 the absorption bands between

1000 and 1200 cm^{-1} were characteristics –C–O– stretching of polysaccharide skeletons. In Sucrose stabilized Fe_3O_4, the two peaks appearing at 1522 and 1382 cm^{-1} correspond to the symmetrical and asymmetrical stretching vibrations of the carboxylate groups [24]. The above mentioned peaks both in Sucrose and Glucose also found to be shifted and the characteristic peaks of Fe_3O_4 at 578 and 626 cm^{-1} appeared in FTIR spectra of FF and GF, suggested that there must be strong vibrational interaction between Fe_3O_4 and polysaccharide.

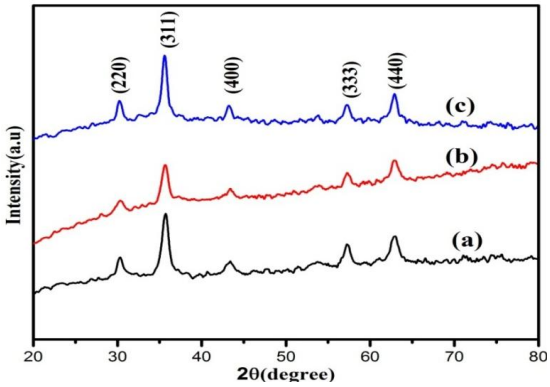

Fig. 1: XRD pattern of (a) GF (b) FF and (c) SF.

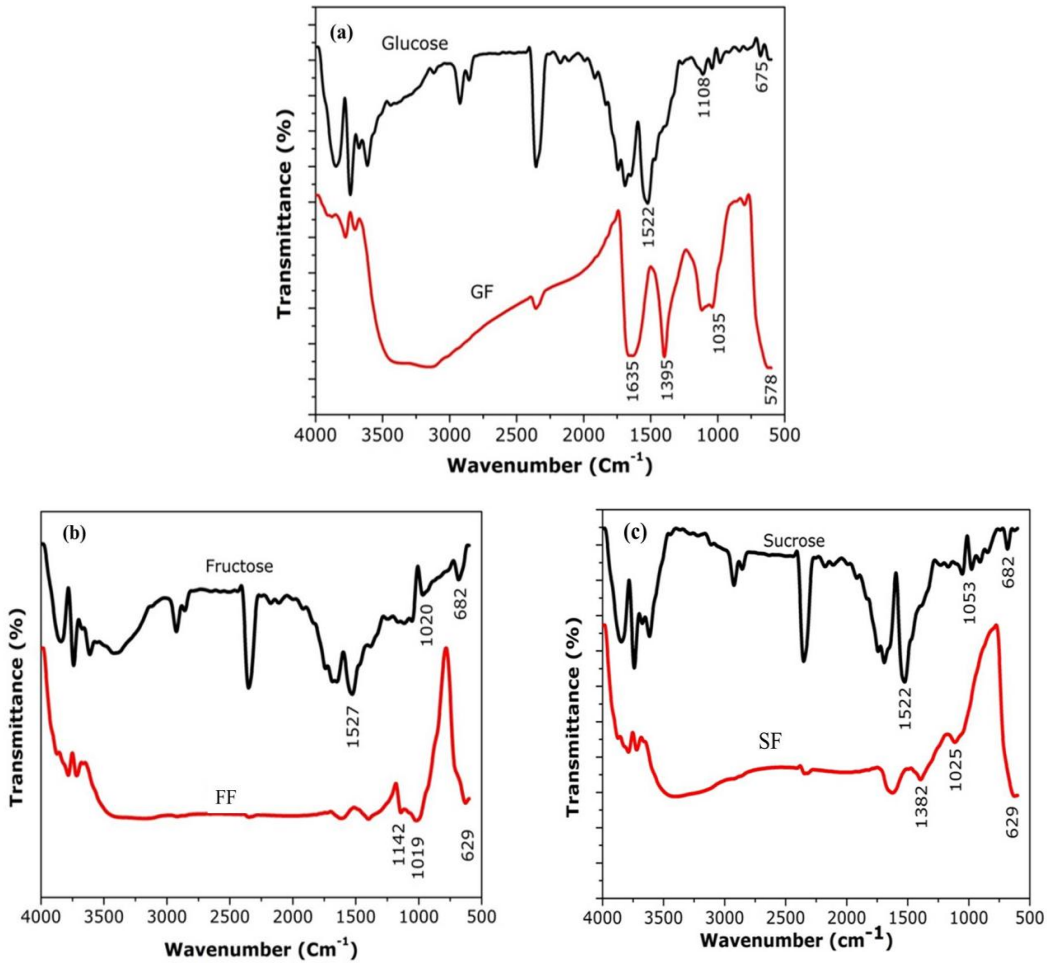

Fig. 2: FTIR spectra of (a) GF (b) FF and (c) SF.

Optical properties

The UV-Vis NIR absorption spectrum was studied to investigate the polysaccharide coating effect on optical absorption and band gap of magnetic nanoparticles. The optical absorption spectra are shown in Fig. 3(a-c) in the wavelength range of 200-2500 nm. The synthesized nanopowders have been dispersed on a glass plate with the aid of insoluble solvent upon drying dispersed nanoparticles have been scanned using UV-Vis NIR lamps. Using absorption data, absorption coefficient (α) was calculated for each value.

Finally graph is plotted between $(\alpha h\nu)^2$ Vs $h\nu$ so as to obtain the E_g value of nanoparticles. The synthesized samples do not reveal sharp absorption edges in UV region. The optical band gap energies of the obtained samples have been determined using Tauc's plot using a relation $\alpha h\nu = A(h\nu - E_g)^2$ and they are shown in Fig. 3 (d-f), in which α is the absorption coefficient, A is a constant, h is Planck's

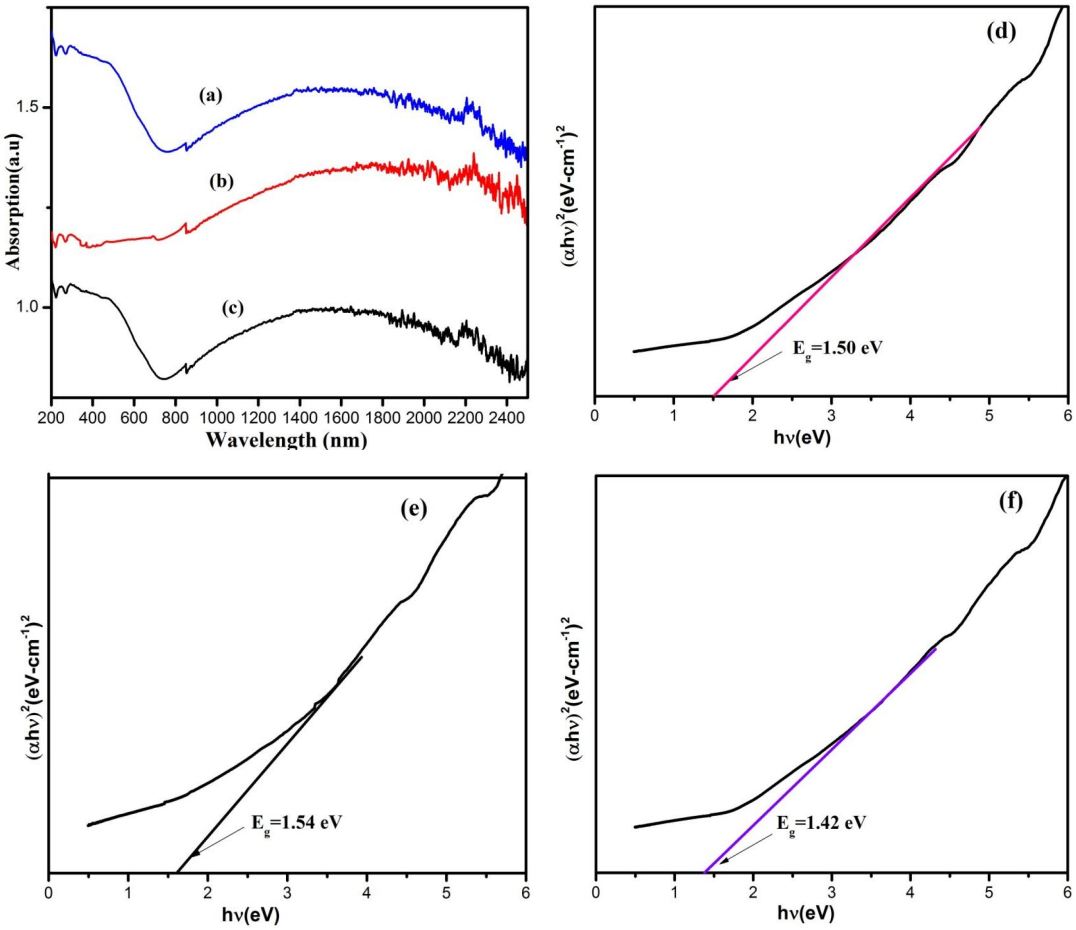

Fig. 3: UV–Vis NIR absorption spectra of (a) GF (b) FF and (c) SF, Plots of (αhν)2 versus hν - indirect transition for (d) GF (e) FF and (f) SF.

Table 1: The Particle size obtained from HRTEM and band gap energy (E_g).

Sl. No	Sample code	Average particle size (nm)	E_g(eV)	References
1	GF	7.50	1.50	Present work
2	FF	7.20	1.54	Present work
3	SF	10.46	1.42	Present work
4	Fe_3O_4/alginate	10.50	2.62	[19]
5	Fe_3O_4	10.59	1.92	[26]
6	Zn/ Fe_3O_4	14.92	1.3	[27]

constant, ν is the photon frequency and E_g is the band gap energy [25]. Band gap studies reveal that E_g value of GF, FF and SF is higher than that of pure Fe_3O_4. The indirect bandgap energies are tabulated in Table.1. The variation of particle sizes with respect to stabilizing agent has influenced the bandgap energies of nanoparticles of Fe_3O_4 [26-27].

TEM analysis

Fig. 4 (a-c) shows the High Resolution Transmission electron microscope (HRTEM) images of the Fe_3O_4 nanoparticles which were encapsulated by polysaccharides. It was clearly observed that the nanoparticles exhibit with an unavoidable aggregation due to magnetic character and indicated the mono dispersed and spherical shape of the nanopowders. HRTEM images divulge that the particles were found spherical in shape. The average particle sizes as obtained from the HRTEM micrographs are 7.5, 7.2 and 10.46 nm for GF, FF and SF. Since polysaccharides could bind with metal ions due to their high number of coordinating functional groups (hydroxyl and glucoside groups) [28]. It was noted that the majority of the iron ions appear to be closely associated with the polysaccharide molecules. Therefore nucleation and initial crystal growth of Fe_3O_4 may have occurred preferentially on polysaccharides. In addition, polysaccharides present interesting dynamic supramolecular associations by the facilitated inter and intra-

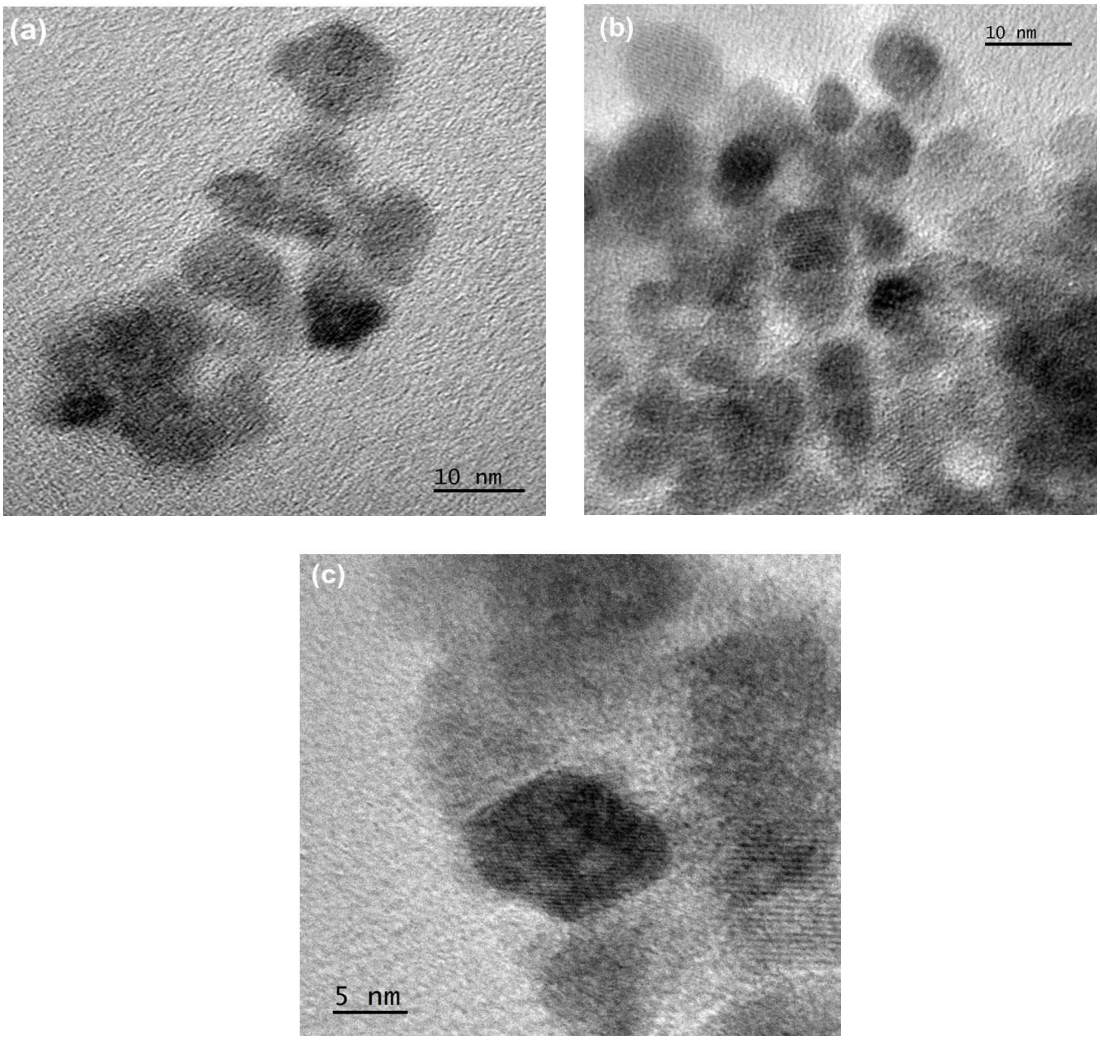

Fig. 4: HRTEM micrographs of (a) GF (b) FF (c) SF.

molecular of hydrogen bonding, which could have acted as the templates for the growth of nanoparticles [29]. Both GF and FF nanoparticles exhibited an approximeately spherical morphology with a mean size less than 7nm, while SF nanoparticles were larger. The particle size results obtained from XRD and HRTEM studies are compared in Table.2 as the earlier results have also been projected.

Magnetization Studies

The magnetic properties of nanoparticles under room temperature condition was studied using a vibrating sample magnetometer and the magnetization values of the samples were systematically recorded as a function of applied magnetic field to an extent of 15000 Gauss. The observed magnetization curves of GF, SF and FF are shown in Fig. 5 (a-c). The insert picture depicts the visual representation of Superparamagnetic in Fe_3O_4 suspension. The hysteresis loop shows no remanance and coercivity upon reducing the field towards the opposite direction. The magnetization curves demonstrate a typical superparamagnetic behavior which shows high susceptibility with saturated magnetization M_s at low filed strength and zero coercivity and remanence.

The values reported in Table 3 show M_s values of 41.69, 42 and 38.43 for GF, SF and FF samples which is much lower than that of bulk magnetite (92 emu/g). The reduced M_s could be attributed to the presence of polysaccharides on the surface of nanospheres, as evidenced from FT-IR studies. In addition, magnetic nanoparticles intrinsically show reduction in magnetization due to the disorder in magnetic spins at surface of the nanoparticles, though particles were well crystalline. The percentage of disordered spins enhances the reduction of particle size due to the increase of surface area to volume ratio [30]. As expected, the squareness ratio for Fe_3O_4 samples stabilized from different media found to be zero in nature.

Fig. 5 (d) show the coercivity as a function of particle size at room temperature. The Gaussian fit of the data shows the increase in size, increases the coercivity and attains a maximum value beyond that the value decreases with size of the particles. From the above it is inferred that the initial increase of the coercivity with the decreasing size further increase due to the enhanced role of the surface and its strong anisotropy. In addition, the single domain effects of cubic magnetite particles have been experimentally observed for smaller dimension particles. The dependence of saturation magnetization on average particle size was also studied and it is shown in Fig. 5 (e). The M_s values obtained for the samples vary between 38 to 42 emu/g. The saturation magnetization increases

Table 2: Comparison of Crystallite size and Particle size.

Sl. No	Sample Code	Particle size (nm)		References
		XRD	HRTEM	
1	GF	3.38	7.50	Present work
2	FF	4.82	7.20	Present work
3	SF	5.23	10.46	Present work
4	Fucan/ Fe_3O_4	10	10	[18]
5	Fe_3O_4/alginate	14	10.5	[19]

Table 3: Magnetic parameters obtained from VSM analysis.

Sl. No	Sample Code	Saturation Magnetization M_s (emu/g)	Coercivity H_c (O_e)	Remanent magnetization M_r (emu/g)
1	GF	41.69	0.55	0.0004
2	FF	38.43	4.42	0.004
3	SF	42	9.13	0.0098

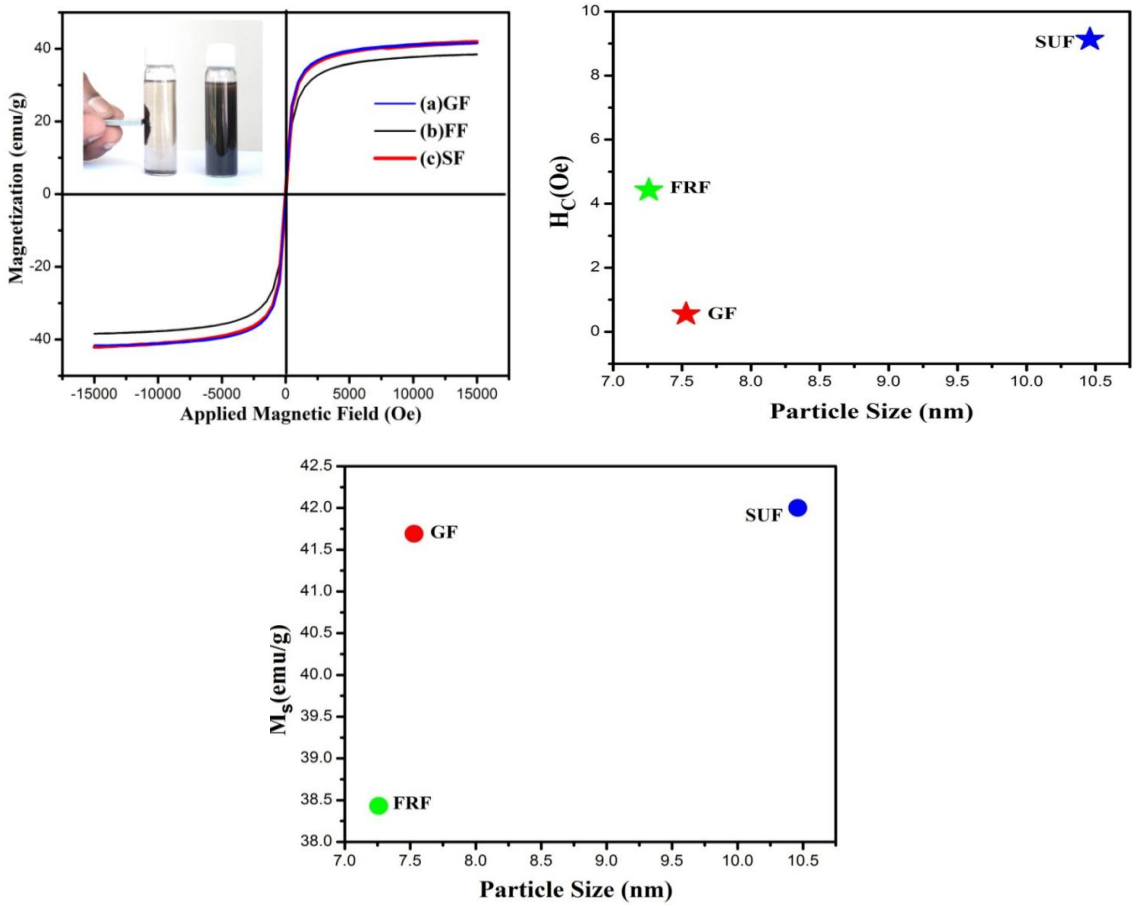

Fig. 5: Magnetization curve of (a) GF, (b) FF, (c) SF, (d) The correlation between the coercivity (H_C) and average particle size (nm), at room temperature and applied field of 15kOe, (e) Saturation magnetization (M_S) as function of average particle size (nm) at maximum applied field of 15kOe.

consistently with size. A very sharp increase in the magnetization between the sizes of 7.53 to 10.46 nm has been obtained while there is a slower increase thereafter as in the case of coercivity disperses with size.

CONCLUSIONS

In summary, magnetic iron oxide nanoparticles stabilized on polysaccharides (Glucose, Fructose and Sucrose) has been synthesized using co-precipitation method. The average nanocrystallite size were found to be 3.3, 4.82 and 5.23 nm from powder XRD and the average particle diameter obtained from HRTEM provides a value 7.53, 7.26 and 10.46 nm for GF, FF and SF respectively. The nanoparticles were single grain in nature. The results showed that the surface modification of Fe_3O_4 nanoparticles by polysaccharide matrix was more effective for the control of size. They also showed superparamagnetic in character at room temperature with reduced saturation magnetization compared to bulk magnetite. In addition, samples possess reasonably saturation magnetization, although FF and SF had slightly larger remanance and coercivity. In general, preparation of nanopowders coated with polysaccharides yields stable, safe, biocompatible and biodegradable magnetic nanoparticle of Fe_3O_4.

ACKNOWLEDGEMENTS

The authors are thankful to Dr. G. Rameshkumar, Department of Physics, University College of Engineering-Arni, 632 326 Tamilnadu, India for fruitful discussions.

CONFLICT OF INTEREST

The authors declare that there is no conflict of interests regarding the publication of this manuscript.

REFERENCES

[1] Duncan R., Spreafico F., (1994), Polymer conjugates. Pharmacokinetic considerations for design and development. *Clin. Pharmacoki*. 27: 290-306.

[2] Boyd B. J., (2008), Past and future evolution in colloidal drug delivery systems. *Exp. Opin. Drug Deliv*. 5: 69-85.

[3] Duncan R., (2007), Designing polymer conjugates as lysosomotropic nanomedicines. *Biochem. Soc. Trans*. 35: 56-60.

[4] Hou C. H., Hou S. M., Hsueh Y. S., Lin J., Wu H. C., Lin F. H., (2009), The in vivo performance of biomagnetic hydroxyapatite nanoparticles in cancer hyperthermia therapy. *J. Biomater*. 30: 3956-3960.

[5] Predoi D., Kuncser V., Zaharescu M., Keune W., Sahoo B., Valeanu M., Crisan M., Raileanu M., Jitianu A., Filoti G., (2004), Structural and magnetic properties of iron species/ SiO_2 nanocomposites obtained by sol–gel methods. *Phy. Stat. Solid*. 1: 3507-3510.

[6] Kang Y. S., Risbud S., Rabolt J. F., Stroeve P., (1996), Synthesis and characterization of nanometer-size Fe_3O_4 and γ-Fe_2O_3 particles. *Chem. Mater*. 8: 2209-2211.

[7] Fried T., Shemer G., Markovich G., (2001), Ordered two-dimensional arrays of ferrite nanoparticles. *Adv. Mater*. 13: 1158-1161.

[8] Jitianu A., Raileanu M., Crisan M., Predoi D., Jitianu M., Stanciu L., Zaharescu M., (2006), Fe_3O_4-SiO_2 nanocomposites obtained via alkoxide and colloidal route. *J. Sol–Gel Sci. Tech*. 40: 317-323.

[9] Predoi D., Crisan O., Jitianu A., Valsangiacom M. C., Raileanu M., Zaharescu M., (2007), Iron oxide in a silica matrix prepared by the sol–gel method. *Thin Sol. Film*. 515: 6319-6323.

[10] Guo S., Li D., Zhang L., Li J., Wang E., (2009) ,Monodisperse mesoporous superparamagnetic single-crystal magnetite nanoparticles for drug delivery. *J. Biomat*. 30: 1881-1889.

[11] Zhang L. Y., Zhu X. J., Sun H. W., Chi G. R., Xu J. X., Sun Y. L., (2010), Control synthesis of magnetic Fe_3O_4–chitosan nanoparticles under UV irradiation in aqueous system. *Current Appl. Phys*. 10: 828-833.

[12] Ding J., Tao K., Li J., Song S., Sun K., (2010), Cell-specific cytotoxicity of dextran- stabilized magnetite nanoparticles. *Colloids and Surf. B: Biointerfaces*. 79: 184-190.

[13] Batalha I. L., Hussain A., Roque A. C. A., (2010), Gum arabic coated magnetic nanoparticles with affinity ligands specific for antibodies. *J. Mol. Recog*. 23: 462-71.

[14] Pourjavadi A., Hosseini S. H., Seidi F., Soleyman R.., (2013), Magnetic removal of crystal violet from aqueous solutions using polysaccharide based magnetic nanocomposite hydrogels. *Poly. Int.* 62: 1038-1044.

[15] Xiao Q., Tan X., Ji L., Xue J., (2007), Preparation and characterization of polyaniline/nano-Fe_3O_4 composites via a novel Pickering emulsion route. *Synth. Meta*ls. 157: 784-791.

[16] Kim G. C., Li Y. Y., Chu Y. F., Cheng S. X., Zhuo R. X., Zhang X. Z. (2008), Nano- sized temperature-responsive Fe_3O_4-UA-g-P(UA-co-NIPAAm) magnetomicelles for controlled drug release. *Europ. Polym. J.* 44: 2761-2767.

[17] Wang Y. M., Cao X., Liu G. H., Hong R. Y., Chen Y. M., Chen X. F., Li H. Z., Xu B., Wei D. G., (2011), Synthesis of Fe_3O_4 magnetic fluid used for magnetic resonance imaging and hyperthermia. *J. Magnetis. Magnetic. Mater.* 323: 2953-2959.

[18] Silva V. A. J., Andrade P. L., Silva M. P. C., A. Bustamante D., Luis De Los Santos V., Albino Aguiar J., (2013), Synthesis and characterization of Fe_3O_4 nanoparticles coated with fucan polysaccharides. *J. Magnetis. Magnetic. Mater.* 343: 138-143.

[19] Manish S., Jay S., Madhu Y., Dinesh Kumar G., Mishra R. K., Shipra T., Animesh K. O., (2012), Synthesis of superparamagnetic bare Fe_3O_4 nanostructures and core/ shell (Fe_3O_4/alginate) nanocomposites. *Carbohyd. Polym.* 89: 821-829.

[20]Cullity B. D, Stock S. R., (2001). Elements of X-ray Diffraction, *New Jersey*.

[21] Chang P. R., Yu J. G., Ma X. F., (2009), Fabrication and characterization of Sb_2O_3/carboxymethyl cellulose sodium and the properties of plasticized starch composite films. *Macromol. Mater. Eng.* 294: 762-767.

[22] Luo X. G., Liu S. L., Zhou J. P., Zhang L. N., (2009), In situ synthesis of Fe_3O_4/cellulose microspheres with magnetic-induced protein delivery. *J. Mater*. *Chem.* 19: 3538-3545.

[23] Laudenslager M. J., Schiffman J. D., Schauer C. L., (2008), Carboxymethyl chitosan as a matrix material for platinum, gold, and silver nanoparticles. *Biomacromol*. 9: 2682–2685.

[24] Rosca C., Popa M. I., Lisa G., Chitanu G. C., (2005), Interaction of chitosan with natural or synthetic anionic polyelectrolytes. 1. The chitosan–carboxymethyl–cellulose complex. *Carbohyd. Poly*. 62: 35-41.

[25] Koteeswara Reddy N., Ramakrishna Reddy K. T., (2006), Optical behavior of sprayed tin sulphide thin films. *Mater. Res. Bull*. 41: 414-422.

[26] Ghandoor H. El, Zidan H. M., Khalil M. M. H., Ismail M. I. M., (2012), Synthesis and some physical properties of magnetite (Fe_3O_4) nanoparticles. *Int. J. Electrochem. Sci.* 7: 5734-5745.

[27] Rezay Marand Z., Helmi Rashid Farimani M., Shahtahmasebi N., (2014), Study of magnetic and structural and optical properties of Zn doped Fe_3O_4 nanoparticles synthesized by co-precipitation method for biomedical application. *Nanomed. J*. 1: 238-247.

[28] Taubert A., Wegner G., (2002), Formation of uniform and monodisperse zincite crystals in the presence of soluble starch. *J. Mater. Chem.* 12: 805–807.

[29] Raveendran P., Fu J., Wallen S. L., (2003), Completely Green synthesis and stabilization of metal nanoparticles. *J. Am. Chem. Soc*. 125: 13940-13941.

[30] Caizer C., (2015), Nanoparticles Size Effect on Some Magnetic Properties. *Springer International Publishing,* 475-519.